Contrib. Astron. Obs. Skalnaté Pleso **44**, 119 – 129, (2014)

White-light corona and solar polar magnetic field strength over solar cycles

V. Rušin, M. Saniga and R. Komžík

Astronomical Institute of the Slovak Academy of Sciences
059 60 Tatranská Lomnica, The Slovak Republic

Received: July 4, 2014; Accepted: October 22, 2014

Abstract. We discuss the large-scale structure of the solar corona, in particular its helmet streamers, as observed during total solar eclipses around maxima of solar cycles and make its comparison with solar polar magnetic field strength as observed by the Wilcox Solar Observatory (WSO) since 1976. Even though the magnetic field strength at the solar poles around cycle minima decreased minimally twice in the last forty years, distributions of helmet streamers around the Sun in different cycles around cycle maxima remain nearly the same. This indicates that large-scale magnetic structures governing the shape and evolution of helmet streamers must be of a different nature than those related with solar polar fields.

Key words: Sun – white-light corona – solar polar magnetic fields

1. Introduction

The structure of the white-light corona has been of great interest for solar physicists since its very first observations during total solar eclipses. At the beginning, coronal structures were just given a descriptive appraisal. In 1928, the so-called flattening index was introduced by Ludendorff (1928) and then also the total brightness of the corona was adopted as an important structural parameter. The total brightness of the visible corona, determined at the heights between 1.03 and 6.00 solar radii, gets its main contributions from two components: K-corona and F-corona. Brightness of the F-corona (I_F), which is prominent at the height above 3 solar radii and arises from scattered sunlight on interplanetary dust, was first described by Grotrian (1934); its light is unpolarized. Brightness of the K-corona (I_K) is due to Thomson scattered emission by free electrons in the solar corona (van de Hulst, 1950); its light is polarized. Both types of brightness are integrated along the line of sight. Contributions of coronal emission lines are neglected. Nowadays, one also speaks of the corona during cycle maxima, cycle minima and the intermediate corona, the three coronas differing in the distribution of helmet streamers which, respectively, are seen around the whole solar disk, only in the vicinity of the solar equator, and both at the equator and mid-latitudes. The understanding of the structure of the white-light corona and its variations over time was already one of central questions for the first observers. The start of the cosmic era gave fresh impetus to the issue, as the Soviet spacecraft *Luna 1* in 1959 confirmed the existence of solar wind (Gringauz et al., 1962) predicted theoretically by Parker a year earlier (Parker, 1958). As solar wind is continuously fed by particles originating in the solar corona, and the latter is shaped by mechanisms of the solar dynamo (Charbonneau, 2010), the study — both ground-based and space-borne — of the large-scale structure of the white-light corona is vital not only for getting insights into the intricacies of origin and distributions of solar magnetic fields, but also for ascertaining the influence of solar wind on the Earth.

In the present paper, we analyze the structure of the maximum type white-light corona as inferred from ground-based observations carried out during total solar eclipses in the period from 1980 to 2013 and make its comparison with temporal variation of solar polar magnetic fields provided by WSO. Remarkably, the average strength of polar magnetic fields features a slight decline since the onset of their measurements in 1976. An interesting question then emerges whether this decline has a discernible imprint on distributions and the number of helmet streamers around the solar disk. It is known (for example, Schatten et al., 1978) that solar polar magnetic fields are recreated by global-scale flows, e.g. meridional flow and differential axi-symmetric rotation, which transport magnetic flux, represented by sunspots in low latitudes, from lower latitudes to polar regions, and that the speed of these flows is variable (and complicated) in time as discussed, for example, by Muñoz-Jaramillo et al. (2010), Zhao, Kosovichev and Bogart (2014), and Upton and Hathaway (2014).

2. Observations

The measurements of solar polar magnetic fields at WSO are available from 1976 up to now and their plot is given in Figure 1. Within the period in question, we have at our disposal seven different series of high-quality eclipse white-light corona observations, whose basic characteristics are summarized in Table 1 and whose corresponding large-scale coronal structures are depicted in Figure 2; to make a picture more complete, we also show in Figure 3 the structure of the corona as seen by SOHO/C2, but only for four different eclipse days.

3. Analysis and results

In our analysis, we shall focus on three major parameters characterizing properties of the white-light corona: its flattening index, total brightness and the distribution of prominent structures.

3.1. Flattening index

As already mentioned in the introduction, the flattening index is one of the first parameters used to characterize the shape of the white-light corona. In

Table 1. An overview of eclipse white-light corona observations; R is the sunspot number for the month of the eclipse and ϵ stands for the flattening index.

Date	Cycle maximum	R	ϵ	Observer
1980, Feb 16	C 21: Dec 1979	155.0	0.03	V.R. and P. Zimmermann
1990, Jul 22	C 22: Jul 1989	149.4	0.04	E. Marková team (priv. comm.)
1991, Jul 11	C 22: Jul 1991	173.7	0.00	E. Royer (priv. comm.)
1999, Aug 11	C 23: Mar 2000	93.7	0.04	V.R. and P. Zimmermann
2001, Jun 21	C 23: Mar 2000	134.0	0.07	F. Dorst (priv. comm.)
2012, Nov 13	C 24: Jan 2014 (?)	61.8	0.01	K. Shiota (priv. comm.)
2013, Nov 03	C 24: Jan 2014 (?)	77.6	0.04	V.R.

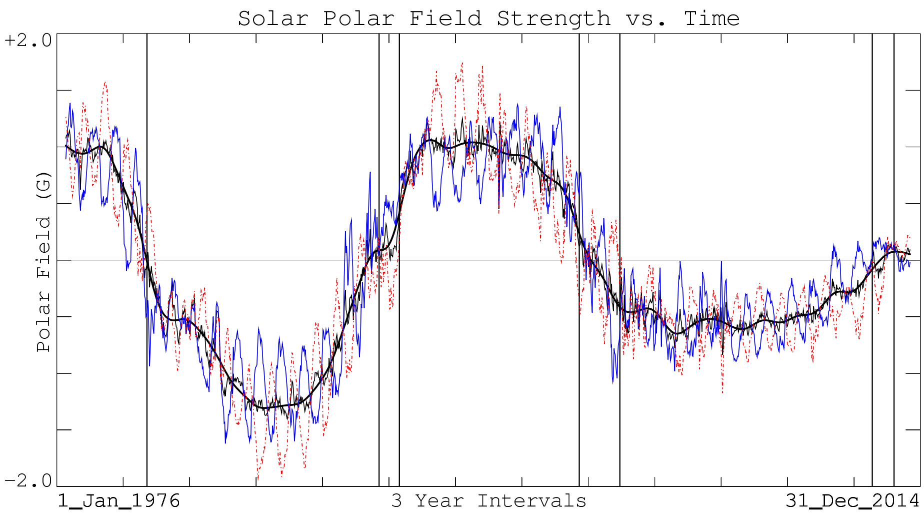

Figure 1. A plot of solar polar magnetic strength vs time (downloaded from WSO's web site `http://www.solen.info/solar/polarfields/polar.html`) and the corresponding values for the times of total eclipses (highlighted vertical lines) given in Table 1. (Key: Lt. Solid = North; Dashed = –South; Med. Solid = Average: (N–S)/2; Hvy. Solid = Smoothed Average)

a recent work, Pishkalo (2011) collected available observations of the corona within the past 150 years and created a figure showing the dependence of the flattening index on the phase of a solar cycle. This figure is reproduced in Figure 4 below, where we supplied a couple of values for eclipse corona in 2012 and 2013.

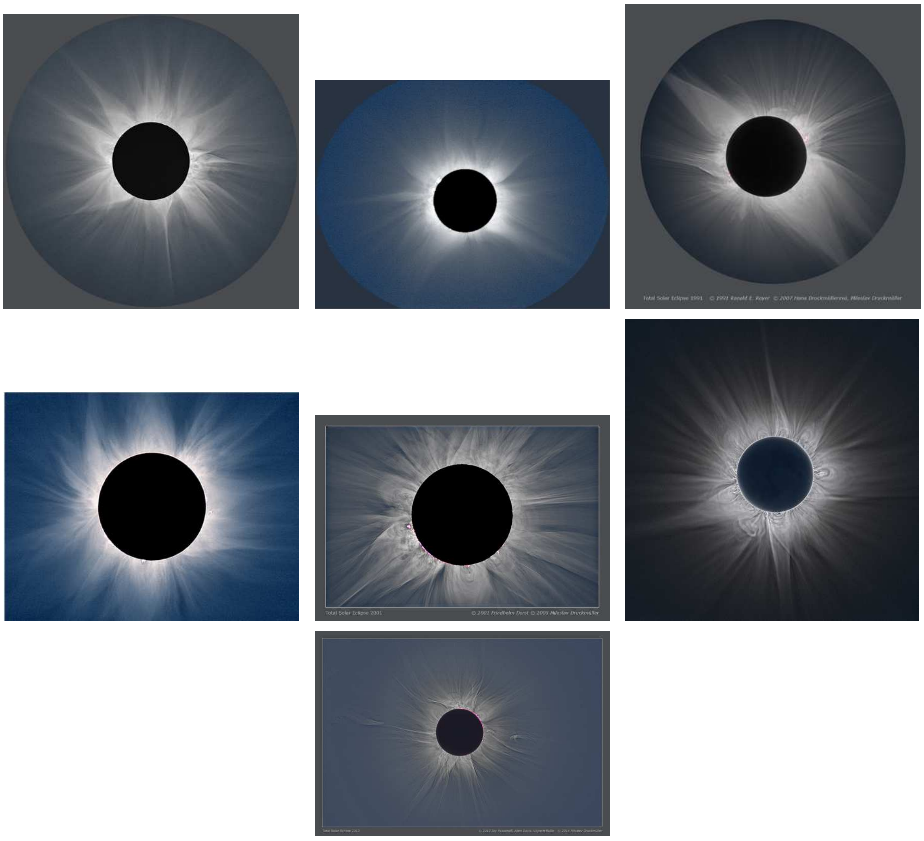

Figure 2. Large-scale structures of the white-light corona on the images processed by Druckmüller's method (Druckmüller et al., 2006, and Druckmüller, 2009). Top (left to right): February 16, 1980; July, 22 1990; and July 11, 1991; middle: August 11, 1999; June 21, 2001, and November 13, 2012; bottom: November 3, 2013.

Whereas the 2012 eclipse took place in the period between the first (November 2011) and second (January 2014) maxima of the cycle, which was characterized by a considerable drop of sunspot number, the 2013 eclipse occurred close to the second maximum, when the value of sunspot number was about 20% higher than that in 2012. Nevertheless, the corresponding values of the flattening index are almost identical (0.02 resp. 0.04) and fit well into the relationship found by Pishkalo. Although the average value of the solar polar magnetic fields in cycle 23 was about one half of that in cycle 22, the flattening index of the white-light corona does not seem to reflect this fact (Pishkalo, 2011).

Table 2. An overview of TBSC. The columns, left to right, give the date of eclipse, phase of the cycle, number of observations (#), the TBSC (in 10^{-6} of the total brightness of the Sun), the sunspot number for the month of the eclipse (R), the flattening index (ϵ) and relevant references.

Eclipse	Phase	#	TBSC	R	ϵ	References
August 30, 1905	0.32	2	0.52	60.2	0.02	Shklovskij (1962)
January 3, 1908	0.51	1	0.95	51.7	0.08	Shklovskij (1962)
June 8, 1918	0.48	1	1.19	92.9	0.23	Shklovskij (1962)
September 21, 1922	0.91	1	0.79	10.4	0.23	Shklovskij (1962)
January 24, 1925	0.14	3	1.03	28.9	0.13	Shklovskij (1962)
January 14, 1926	0.24	1	1.24	59.9	0.07	Shklovskij (1962)
May 9, 1929	0.59	1	0.88	63.4	0.12	Abbott (1955)
June 19, 1936	0.26	2	1.19	78.7	0.06	Shklovskij (1962)
June 8, 1937	0.36	2	1.15	111.6	0.09	Shklovskij (1962)
September 21, 1941	0.77	1	0.76	46.9	0.30	Shklovskij (1962)
July 9, 1945	0.14	1	0.90	37.8	0.32	Abbott (1955)
February 25, 1952	0.79	1	0.79	43.4	0.27	Ru & Ry (1985)
June 30, 1954	0.02	1	0.48	7.0	0.32	Ru & Ry (1985)
February 15, 1961	0.65	1	0.73	74.7	0.17	Ru & Ry(1985)
February 5, 1962	0.75	1	1.09	44.3	0.27	Ry & Ru (1985)
February 5, 1962	0.75	1	1.05	44.3	0.27	Ru & Ry (1985)
July 20, 1963	0.88	1	1.12	26.4	0.28	Ru & Ry (1985)
May 30, 1965	0.05	1	0.68	15.4	0.24	Ry & Ru (1985)
November 12, 1966	0.18	1	0.92	66.9	0.31	Ry & Ru (1985)
September 22, 1968	0.34	1	1.42	107.7	0.06	Ry & Ru (1985)
September 22, 1968	0.34	1	0.35	107.7	0.06	Dzyubenko et al. (1971)
June 30, 1973	0.74	1	0.84	39.4	0.27	Ry & Ru (1975)
June 30, 1973	0.74	1	0.64	39.4	0.27	Vsekhsvyatskij et al. (1981)
October 23, 1976	0.04	1	0.52	15.6	0.36	Dürst (1979)
February 16, 1980	0.34	1	1.29	155.0	0.03	Ry & Ru (1985)
June 21, 2001	0.43	1	1.15	110.9	0.07	Pintér et al. (2003)
August 1, 2008	0.97	1	0.40	2.7	0.30	Hanaoka et al. (2012)
July 22, 2009	0.06	1	0.40	3.6	0.24	Hanaoka et al. (2012)

In "References": Ru = Rušin, Ry = Rybanský

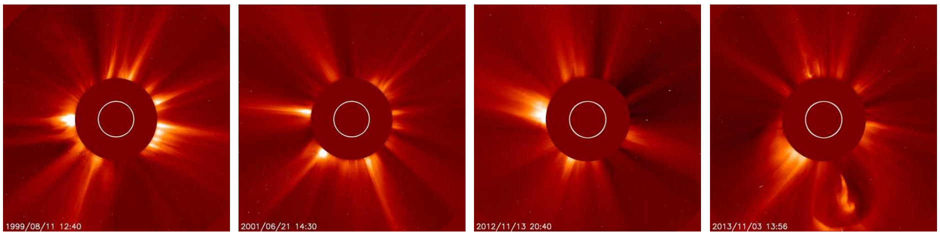

Figure 3. Large-scale white-light coronal structures as seen by SOHO in 1999, 2001, 2012 and 2013 for the days of the eclipse observations. The N-pole is up. (ESA/NASA/SOHO/C2).

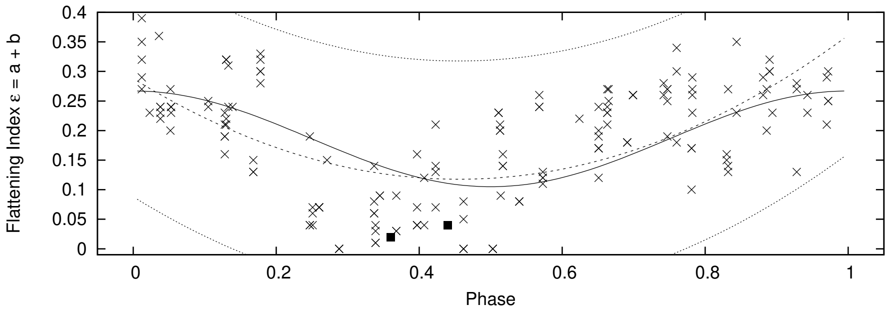

Figure 4. A plot of the flattening index vs solar activity phase (after Pishkalo, 2011). The two additional values represented by filled squares correspond to the 2012 and 2013 eclipses. The length of cycle 24 was estimated to be 11.0 years, its onset being in December 2008.

3.2. Total brightness of the solar corona

The dependence of the brightness of the corona on sunspot number was noticed as early as the end of the 19th century (see, e.g., Pishkalo, 2011, and references therein) and its variation with the phase of a solar cycle is also a fairly-discernible fact (e. g., Rušin, 2000, and references therein). Nowadays, we use the term total brightness of the solar corona (TBSC) and its values are inferred from observations at the heights ranging from 1.03 solar radii to 6.00 solar radii above the solar limb (see, e. g., Rušin and Rybanský, 1985, and/or Rušin, 2000). Although measurements of TBSC during eclipses are rather sparse, we did a search in available literature and found 28 different values pertaining to 25 total solar eclipses in the period from 1905 to 2010, as summarized in Table 2. The dependence of TBSC on the phase of a solar cycle is illustrated in Figure 5.

It is worth mentioning that the smallest values of TBSC ever measured are those of Hanaoka et al. (2012) for the total solar eclipses on 1 August 2008

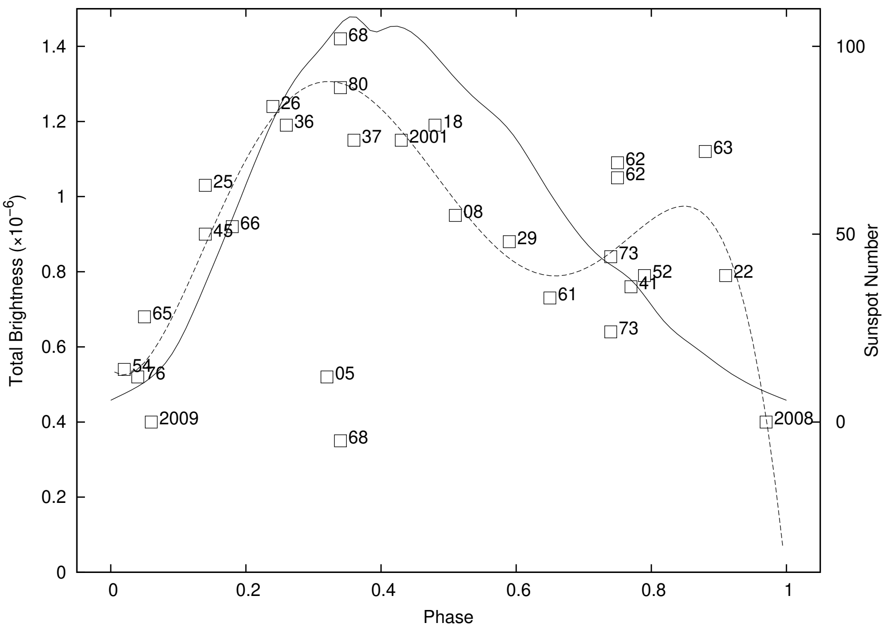

Figure 5. The total brightness of the white-light corona as a function of the phase a solar cycle. The solid line represents an averaged sunspot number of cycles 1 to 22 (Hathaway, 2010); the dashed line is the fit by a fifth-order polynomial (the values for 1905 and 1968 were omitted in these calculations). The years for each eclipse are given next to the symbols.

and 22 July 2009, when solar activity was at its lowest in one hundred years; for both eclipses they got approximately the same value, 0.40 $\times 10^{-6}$ of the total brightness of the Sun. Before, the record was held by the value of 0.48 $\times 10^{-6}$ of the total brightness of the Sun from the time close to the minimum of solar cycle in 1954. Unfortunately, no values of TBSC are available for the total eclipse corona of 2012 and 2013. However, using an empirical relation between the flattening index (f) and TBCS (J_K) proposed by Rušin and Rybanský (1985),

$$f = 0.364 J_K + 0.514,$$

one gets for the 2012 and 2013 eclipses the reasonable estimates of 1.302 $\times 10^{-6}$ and 1.457 $\times 10^{-6}$ of the total brightness of the Sun, respectively.

The inferences drawn from Figure 5 for the TBSC might, at first sight, seem somewhat contradictory. Insofar as the maximum sunspot number is related to the solar polar field strength at the preceding minimum (e.g., Schatten et al., 1978), one would expect there to be a relationship between TBSC (at maximum) and solar polar field strength (at the preceding minimum), just as there is a relationship between TBSC and the sunspot number over the 11-yr cycle. As a result, we would expect to see more variation in TBSC values between big cycles and small cycles at solar maximum than is apparent in Figure 5. There is a hint of this for the discounted cycle 1905 (not considered in the analysis for Figure 2) but the derived TDSC values for 2012 and 2013 are comparable to those of larger cycles. In general, however, the relative independence of coronal structure at solar maximum on the solar polar field strength should not be surprising, simply because the polar fields, whatever their strength at the preceding maximum, disappear at solar maximum and all that is left to control the coronal structure is the toroidal sunspot fields which are carried poleward by diffusion and meridional flow. While the solar polar fields have a clear effect on coronal structure at solar minimum, they have relatively little effect on TBSC at 11-yr minima. This can be seen from a consideration of the three lowest values of TBSC (discounting the values in 1905 and 1968) in Figure 1, which occurred in 2008, 2009, and 1954. The sunspot numbers for 2008, 2009, and 1954 were 2.9, 3.1, and 4.4, respectively (the smallest values near minima for the time span of the eclipses in Table 2), while the inferred polar fields for 1954, preceding the largest cycle of the modern era, would be much larger than those observed in 2008/2009 which preceded the smallest cycle of the space age. The large difference in polar field strength between the 1954 and 2008/2009 minima made little difference in TBSC values at these times which were controlled by the similar sunspot numbers.

To finish this section, we would like to stress that a precise evaluation of TBSC is a rather intricate and formidable task, as also pointed out by Hanaoka et al. (2012) for eclipse observations and/or Morgan and Habbal (2007) for observations carried out by SOHO. A nice illustration of this fact is the total solar eclipse in 1968, where two different groups of observers arrived at the values of 0.38 and 1.42 $\times 10^{-6}$ of the total brightness of the Sun.

3.3. Large-scale structure of the white-light corona

Already after the first few eclipse observations it was obvious that the shape and structure of the corona is not stable, but varies considerably over time, and hence with the phase of a solar cycle. Basically, there are two different kinds of dominant structures seen almost anytime in the corona: helmet streamers and coronal holes. Helmet streamers are prominent loop-like structures with long pointed peaks that connect regions of opposite magnetic polarity. Coronal holes are large dark regions seen in extreme ultraviolet and/or X-ray images of the Sun; although they may appear any time during the solar cycle, they are most prominent at the poles during cycle minima in the white-light corona.

As we deal with the white-light corona, we shall only be concerned here with helmet streamers, whose distribution also varies within a solar cycle. During cycle minima, when the large-scale magnetic fields of the Sun have a pronounced dipole character, they are mostly located around the equator, whereas during cycle maxima they are seen around the whole solar limb. Helmet streamers are usually confined to the streamer belt in the mid-latitudes, and their migration pattern during a cycle seems to follow that of prominences/active regions (see, e. g., Waldmeier, 1963, Rušin, 2000, and/or Bělík et al., 2004). On the other hand, the large scale structure of the corona as represented by helmet streamers does not develop chaotically. The topology of helmet streamers is well described by a distribution of magnetic field lines, e.g. Low (1996), as measured in the photosphere. We note, present techniques do not allow measure their strength directly in the corona. Distributions of helmet streamers within different cycles also depend, after Waldmeier (1963), upon the position of stationary prominence zones, whose arrival to the poles correlates with sunspot number and differs between high and low magnitude of the cycle. We also note that Wang et al. (2007) even speak about two different kinds of helmet streamers: (a) classical helmet streamers that separate coronal holes of opposite magnetic polarity and (b) pseudostreamers that overlie twin loop arcades and separate holes of the same polarity.

Given these facts, it is of some importance to ask whether there is a noticeable correlation between the occurrence of helmet streamers and the strength of solar polar magnetic fields. As already pointed out in Sec. 1 based on the plot given in Figure 1, the maximum values show continuous decline, the latest value being about a half of that first measured. However, if we go through processed images of the white-light corona shown in Figure 2, we do not see any big difference between them as per occurrence and distribution of helmet streamers. The only exception is eclipse in 1991 when the flattening index was almost zero, but the shape of the white-light corona did not answer to this fact, which might have been caused by an unusual position/orientation of the heliomagnetic sheet to the rotational axis of the Sun. Hence, we did not see evidence that the distribution of helmet streamers reflects the fact of continuously declining maximum values of polar magnetic field strength. An explanation of this behavior can lie with the fact that the eclipse in July 1991 appears to have occurred when the polar fields had begun to recover following polarity reversal but, of course, the phasing should be checked in detail for this and the other events. If the polar fields have recovered sufficiently, this will flatten the high-latitude streamers so that they become more parallel to the equator rather than radial as observed.

4. Concluding remarks

As it is well known (e. g., Rušin and Rybanský, 2002), the corona emission spectral line of 530.3 nm, whose intensity depends approximately on the square of the local density of electrons and temperature (higher than 1.5×10^6 K), is sensitive to variations of local magnetic fields in the photosphere. The coronal density enhancements tend to be strongest in sunspot zones which fall very roughly between $\pm 45°$, where coronal particles are trapped by the strong magnetic fields (coronal loops). In the period from 1976 to 1999 it was found that the higher the strength of local magnetic fields, the higher the intensity of this line. A similar dependence was also found, in the period from 1979 to 2014, for the so-called MgII-index (`http://www.iup.physik.uni-bremen.de/gome/gomemgii.html`). Our findings concerning the abundance and distributions of helmet streamers are thus in contrast with the above facts, as are our recent findings concerning the average widths of the bases of helmet streamers that also do not seem to show any significant variation with either the phase of a solar cycle or the strength of local magnetic fields (Rušin et al., 2013; in this respect, see also Merzlyakov and Starkova, 2012). Similarly, from our data it follows that there is no discernible dependence of the flattening index on the maximum strength of solar polar magnetic fields. This may serve as a justification of recent results of Kramar et al. (2014) showing that we are still far away from a proper understanding how large-scale magnetic fields influence a highly complex and variegated structure of the white-light solar corona.

Acknowledgements. This work was supported by the VEGA grant No. 2/0003/13. V.R. participation in the Gabonese eclipse 2013, as a member of the Williams College 2013 total-eclipse expedition, was supported in part by grant 9327-13 from the Committee for Research and Exploration of the National Geographic Society. We are also grateful to our colleagues who obtained high-quality pictures of the eclipse corona, in particular to the Upice Observatory 1991 eclipse team led by E. Marková, F. Dorst (2001 eclipse), E. Royer (1999 eclipse) and K. Shiota (2012 eclipse), or took part in obtaining the relevant observations, namely P. Zimmermann (the 1980 and 1999 eclipses). We would also like to thank M. Druckmüller for processing the data using his method. Last, but not least, our thanks also go to an anonymous referee for his/her constructive remarks and suggestions.

References

Abbott, W.N.: 1955, *Ann. Astrophys.* **18**, 81

Bělík, M., Marková, E., Rušin, V., and Minarovjech, M.: 2004, *Sol. Phys.* **224**, 269

Charbonneau, P.: 2010, *Living Rev. Solar Phys.* **7**, 3

Druckmüller, M., Rušin, V., and Minarovjech M.: 2006, *Contrib. Astron. Obs. Skalnaté Pleso* **36**, 131

Druckmüller, M.: 2009, *Astrophys. J.* **706**, 1605

Dürst, J.: 1979, *Astron. Mitt. (Zürich)* **256**, 1

Dzyubenko, N.I., Ivanchuk, V.I., Rubo, G.A., and Churyumov, K.I.: 1971, *Soln. Dann.* **6**, 73

Gringauz, K.I., Bezrukikh, V.V., Ozerov, V.D., and Rybchinskii, R.E: 1962, *Planet. Space Sci.* **9**, 97

Grotrian, W.: 1934, *Zeit. Astrophys.* **8**, 124

Hanaoka, Y., Kikuta, Y., Nakazawa, J., Ohnishi, K., and Shiota, K.: 2012, *Sol. Phys.* **279**, 75

Hathaway, D.H.: 2010, *Living Rev. Solar Phys.* **7**, 1

Kramar, M., Airapetian, V., Mikic, Z., and Davila, J.: 2014, *Sol. Phys.* **239**, 2927
Low, B.C.: 1996, *Sol. Phys.* **167**, 217
Ludendorff, H.: 1928, *Sitz-ber. Preuss Akad. Wiss.* **16**, 185
Merzlyakov, V.L., and Starkova, L.I.: 2012, *Geomagnetism and Aeronomy* **52**, 908
Morgan, H., and Habbal, S.R.: 2007, *Astron. Astrophys.* **471**, L47
Muñoz-Jaramillo, A., Nandy, D., Martens, P.C.H., and Yeates, A.R.: 2010, *Astrophys. J.* **720**, L20
Parker, E.N.: 1958, *Astrophys. J.* **128**, 677
Pintér., P., Klocok, Ľ., Minarovjech, M. and Rybanský, M.: 2003, in *Solar Variability as an Input to the Earth's Environment*, ed.: Wilson, A., ASP Conf. Ser. 205, ESA SP 535, 243
Pishkalo, M.I.: 2011, *Sol. Phys.* **270**, 347
Rušin, V.: 2000, in *Last Total Solar Eclipse of the Millennium*, ed.: W. Livingston and A. Özgüc, ASP Conf. Ser. 205, Astronomical Society of the Pacific, 17
Rušin, V., and Rybanský, M.: 1985, *Bull. Astron. Inst. Czechosl.* **36**, 77
Rušin, V., and Rybanský, M.: 2002, *Sol. Phys.* **207**, 47
Rušin, V., Saniga, M., and Komžík, R.: 2013, *Contrib. Astron. Obs. Skalnaté Pleso* **43**, 73
Rybanský, M., and Rušin, V.: 1975, *Bull. Astron. Inst. Czechosl.* **26**, 206
Rybanský, M., and Rušin, V.: 1985, *Bull. Astron. Inst. Czechosl.* **36**, 73
Schatten, K.H., Scherrer, P.H., Svalgaard, L., and Wilcox, J.M.: 1978, *Geophysical Research Letters* **5**, 411
Shklovskij, I.S.: 1962, *Fizika solnechnoj korony*, Gossudar. Izd. Fiz. Mat. Lit., Moskva
Upton, L., and Hathaway, D.H.: 2014, *Astrophys. J.* **780**, 8pp
van de Hulst, H.C.: 1950, *Bull. Astron. Inst. Netherlands* **11**, 135
Vsekhsvyatskij, S., Dzyubenko, N.I., Ivanchuk, V.I., Popos, S.O., Rubo, G.A., Koutchmy, S., and Stellmacher, G.: 1981, *Astron. Zh.* **58**, 376
Waldmeier, M.: 1963, in *The Solar Corona*, ed.: J.W. Evans, IAU Symposium No. 16, New York and London, 129
Wang, Y.-M., Sheeley, N.R., Jr., and Rich, N.B.: 2007, *Astrophys. J.* **658**, 1340
Zhao, J., Kosovichev, A.G., and Bogart, R.S.: 2014, *Astrophys. J., Lett.* **789**, L7